PASSIVE AZIMUTH LOCALIZATION OF DOLPHIN WHISTLES USING ACOUSTICALLY SMALL SENSORS

PF Dobbins Systems Engineering and Assessment Ltd., SEA House, Bristol Business Park, Coldharbour Lane, Bristol, BS16 1EJ, UK
DP Nowacek Florida State University, Department of Oceanography, Tallahassee, Florida 32606-4320 USA

1 INTRODUCTION

Many passive acoustic techniques that might be applied to the acoustic tracking of dolphins are currently under investigation. Several of these are based on single hydrophones [1,2], but such an approach is clearly limited in performance and reliant on appropriate multipath propagation for localization. On the other hand, towed arrays [3,4], distributed sonobuoys [5]or arrays of bottom-mounted sensors [6,7]all represent major logistical operations.

There is clearly a need for an approach between these two extremes, and this paper considers a system known as Pod-Track, which is intended initially for detecting, tracking and possibly identifying individual wild dolphins in very shallow waters near the Florida coast. Initial “proof of concept” trials will be conducted in April/May 2007, principally to provide data for detection and localization algorithm evaluation, but preliminary modelling and simulations have been carried out to give confidence in the array design and the algorithms to be tested.

Acoustic signals emitted by dolphins include echolocation clicks and communication whistles [8,9]. The high frequency and high directivity of echolocation signals means that they are only detectable at short ranges when the dolphin is heading towards the receiver. Whistles are lower in frequency, less directional and as such are detectable at greater distances. Whistles also offer the possibility of distinguishing between individual dolphins [10].

The system is based on a vertical line array (VLA) suspended from a buoy and is compact enough for single-handed deployment from a small boat. It has the gain and directivity to detect dolphin whistles to a range many times greater than a single hydrophone, and to localise in range and depth using existing algorithms [11,12]. Azimuth localisation is achieved with “triplet” hydrophones using processing techniques based on those employed in towed arrays to overcome the left/right ambiguity [13] and that is the main topic of what follows.

2 THE ARRAY

A provisional array design is shown in Figure 1. The vertical array in Figure 1A comprises eight hydrophones uniformly spaced a distance *d* apart. This spacing is chosen to enable unaliased resolution of signals arriving from all possible vertical directions at up to 22.05kHz, the highest frequency recorded with conventional audio equipment. As explained below, the audio range is well matched to dolphin whistles. Propagation modelling suggests that signals arriving at vertical angles outside the range ±15° will be at least 60dB below the direct arrival and can be ignored. The depth of the top hydrophone, *h*, is chosen to place the array at about mid-depth in 2m of water.

The horizontal array in Figure 1B is made up of three hydrophones equally spaced around a circle of radius *r*, chosen so that the array will fit in a standard sonobuoy case, in keeping with the desire to make the system easily deployable from a small boat. As stated above, this configuration is based on “triplets” used in towed arrays [13].

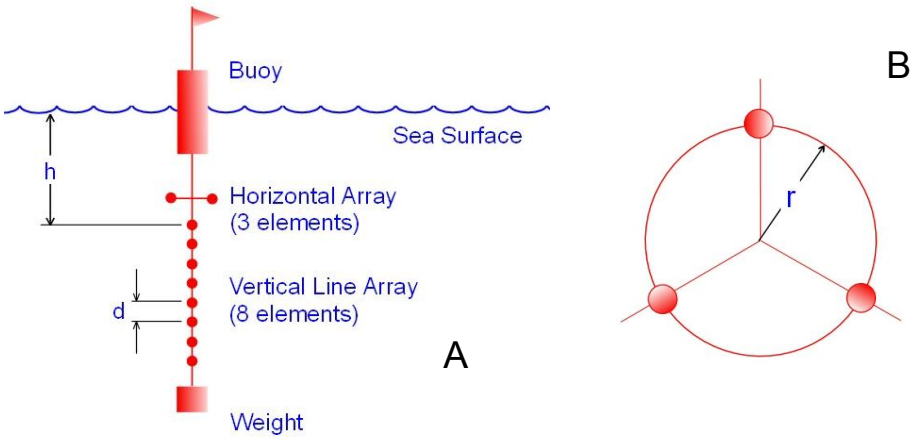

Figure 1. Sketch of outline design for vertical array (A) and azimuth array (B).

The chosen parameters are depth, *h*, 0.86m, spacing, *d*, 0.04m and azimuth array radius, *r*, 0.05m. The vertical spacing of 0.04m is close to optimum for this application, but may not be appropriate for deep-water operation.

3 DOLPHIN WHISTLES

3.1 Whistle Characteristics

The acoustic repertoire of Florida dolphins has been studied extensively, and much of the original research on dolphin whistle production was conducted in Florida [8]. In the decades since, many significant investigations into the use and context of signature whistles have been conducted with wild Florida dolphins [14,15,16]. Thus, there is an ample supply of examples of dolphin whistles recorded in the environment where the system must operate in the first instance.

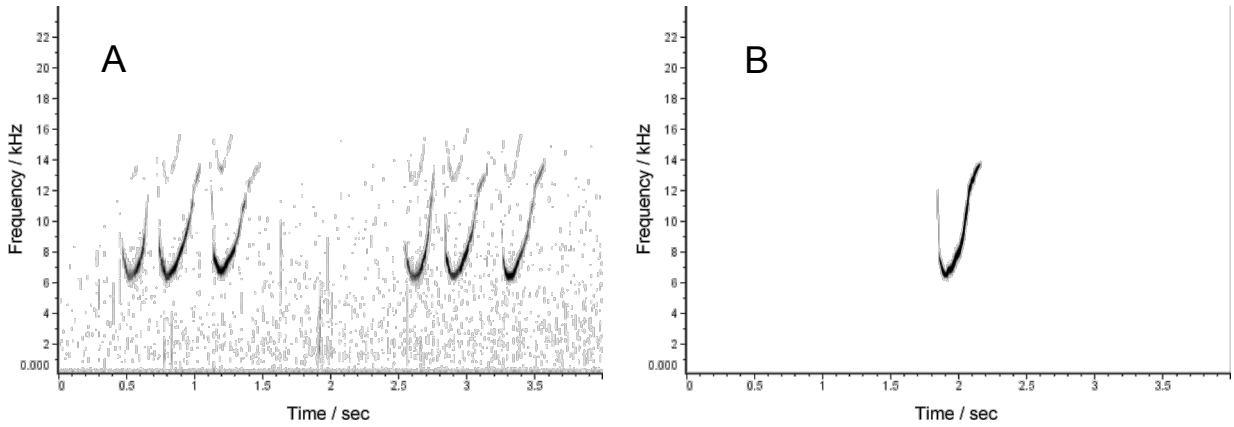

Figure 2. Spectrograms of dolphin whistles from the area of interest. The left hand example is a "clean" signal recorded at short range while the other shows a simulated signal having the same time-frequency contour as the recorded whistles.

The animals of interest are Atlantic bottlenose dolphin, *Tursiops truncatus*, and their whistles typically sweep through a range from about 5kHz to 15kHz following a smooth but irregular time-frequency contour over a period of 0.25 – 1 second. The spectrogram of a sequence of typical whistles is shown in Figure 2A. In Figure 2B is an artificial whistle with a time-frequency contour

derived from the signals shown in the left hand plot, and a smooth (Hanning) envelope. This is the test signal used in the simulations that follow.

3.2 Whistle Detection

Dolphin whistles inherently possess a high BT product, so are amenable to high-gain detection and pulse compression using many conventional signal processing techniques. This allows whistles to be detected even if below the ambient noise level and the arrival time to be identified with a resolution much less than the physical duration of the whistle. The presence of noise, however, will introduce a scatter in the estimate of the arrival time and signal amplitude and Figure 3A shows the variation obtained with the signal of Figure 2 embedded in white noise at –20dB signal to noise ratio(SNR). The detector is a basic matched filter and the peak is located by fitting a parabola to the global maximum in the filter output and two points on either side. The arrival time and amplitude estimates can then be computed from the parabola's coefficients.

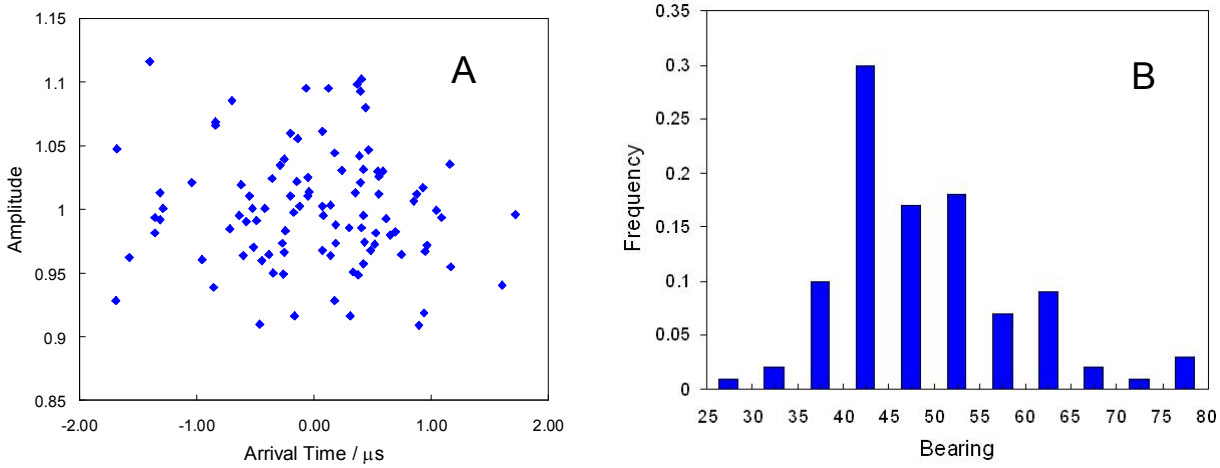

Figure 3. Scatter in time of arrival and amplitude estimates for whistle at –20dB SNR (A) and resulting distribution of bearing estimates obtained using a hyperbolic localization procedure (B)

In this example, obtained from 100 realisations of the simulated noise contaminated whistle, the standard deviation of the variations in arrival time estimates is 0.72 μs, with a spread of about 2 μs. With the array geometry shown in Figure 2B, the maximum difference in arrival time between hydrophones is 57 μs, so this spread represents about 3.5% of the maximum time difference.

The effect this has on the localization performance of a simple hyperbolic procedure [Spiesberger] can be seen in Figure 3B, which shows a histogram of the distribution of bearing estimates for 100 realisations with a source at 42.0° bearing and a range of 500m, with the arrival time at each transducer subject to a random variation with a normal distribution and a standard deviation of 0.72 μs. The mean bearing estimate was 43.9°, an error of 1.9°, with a standard deviation of 9.97°. Although this was a crude test, it is clear that, because the uncertainty in arrival time for dolphin whistles in a noisy background is significant compared with the arrival time difference between array elements, the errors in angular localization obtained from hyperbolic techniques are likely to be unacceptable.

4 CARDIOID ANGULAR LOCALIZATION

During the Second World War Radio Direction Finding (RDF) systems were developed that used a sharp null in the directivity pattern, rather than a peak, to determine the bearing of a signal source. A common technique was to combine a loop antenna, which has a figure-of-eight directivity pattern, with an omnidirectional monopole [17]. The result is a cardioid (heart-shaped) radiation pattern. The

loop is physically rotated until the signal vanishes; the direction of the null then gives the source bearing. This approach gives fine angular resolution with an aperture that is small relative to the wavelength.

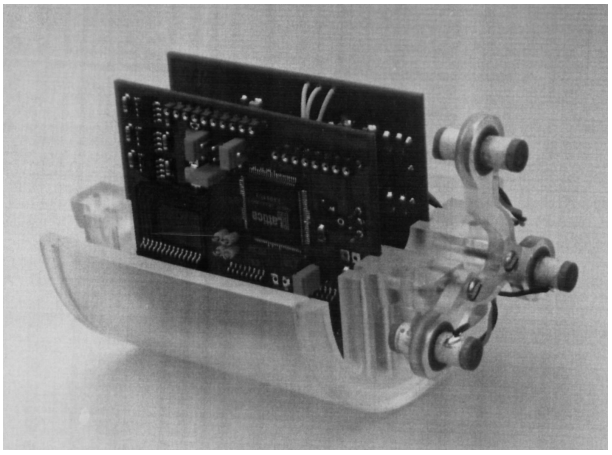

Figure 4. Triplet hydrophone assembly.

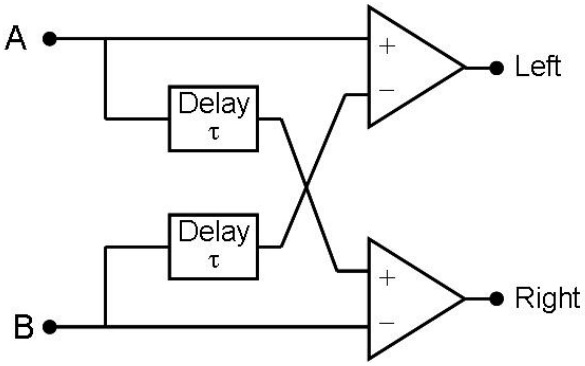

Figure 5. Cardioid formation principle.

Cardioid directivity patterns are also used in towed arrays to discriminate between signals arriving from left and right. In this case, the pattern is obtained using “triplet” hydrophones, as seen in Figure 4, comprising three hydrophones equally spaced around a circle oriented in a vertical plane. A position sensor selects the pair of elements nearest to horizontal and the cardioid pattern is formed by taking the difference between one hydrophone output and a delayed version of the other as shown in Figure 5. If the delay equals the propagation delay between the two elements then a perfect cardioid is obtained.

This method shares the advantage with the loop antenna of achieving a sharp null with a small aperture and it might appear that the triplet could be rotated into the horizontal plane and used to achieve azimuth localization. However, a pair of transducers can only give a single unambiguous null in one direction and the sensitivity to coherent signals falls by 6dB/octave as frequency is reduced while the sensitivity to incoherent noise is constant [13]. This means that broadband signals are distorted and suffer reduced SNR at the bottom of the frequency range.

An alternative is to use all three elements in a conventional beamformer (CBF) configuration as shown schematically in Figure 6A. The weighting coefficients, α_1, α_2, α_3, are understood to be complex and the output from this array may be written

$$V_O = \sum_{n=1}^{3} \alpha_n \left[\cos\left(kr \sin \psi_n \sin \theta\right) + i \sin\left(kr \sin \psi_n \sin \theta\right)\right] \quad (1)$$

Where k is the wavenumber, $2\pi f/c$, f is frequency, c is the sound speed, r is the radius of the triplet array, ψ_n is the angular position of the nth hydrophone and θ is azimuth bearing.

It is necessary to choose the complex weights so that the response V_O has its maximum and nulls in the required directions. However, the real and imaginary terms must be summed separately before the phase and amplitude of the output can be computed. This process can be simplified by applying a conceptual transformation to the array and beamformer architecture []. Figure 6B shows the new configuration. There are still 3 sensors, but each sensor output is split into two virtual channels, one of which is phase shifted by $\pi/2$ so that the co-phase and quadrature components of the weighting coefficients α_n may be individually applied.

The beamformer output may be separated into its real and imaginary parts and each equated to the real and imaginary parts of the desired response in a number of directions. A system of linear equations results that may be solved for the coefficients *A*n, where $\alpha_1 = A_1 + iA_2$ and so on. The set of equations is:

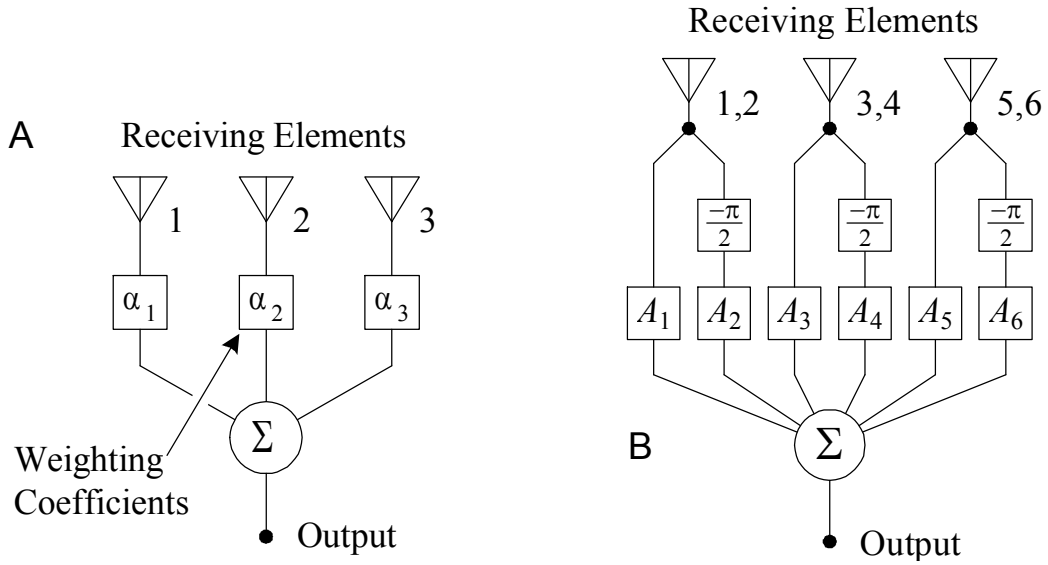

Figure 6. Conventional array and beamforming architecture (A) and "virtual" array architecture (B).

$$\left.\begin{aligned} &A_1 v_{1,1} + A_2 v_{1,2} + \ldots + A_6 v_{1,6} = w_1 \\ &A_1 v_{2,1} + A_2 v_{2,2} + \ldots + A_6 v_{2,6} = w_2 \\ &\cdot \\ &A_1 v_{6,1} + A_2 v_{6,2} + \ldots + A_6 v_{6,6} = w_6 \end{aligned}\right\} \tag{2}$$

$$v_{m,n} = \begin{cases} \cos\left(kr \sin\psi_n \sin\theta\right), & m\text{odd} \\ \sin\left(kr \sin\psi_n \sin\theta\right), & m\text{even} \end{cases} \tag{3}$$

$$w_m = \begin{cases} 1 & \text{, maximum, } m \text{ odd} \\ 0 & \text{, otherwise} \end{cases} \tag{4}$$

These equations are only soluble if the combination of maxima and nulls sought is physically realisable. The simplest way to ensure a result is to use a least-squares approximation to solve Eqs.(2-4). This is straightforward and implemented at a high level in many mathematical software packages, so the details will not be discussed here. Such an approach will attempt to fit the pattern to the specified points, but may not do so exactly. However, the success of the operation is easily determined by inspection.

As an example, Table 1 lists complex coefficients to form a cardioid with the null steered to 195° based on the array geometry in Figure 1. The resulting directivity pattern is shown in Figure 7

Sensor	Real	Imag
1	1.18220	-0.236034
2	-0.346069	0.156413
3	-0.714275	0.449360

Table 1. Example complex coefficients forming a cardioid with null steered to 195°

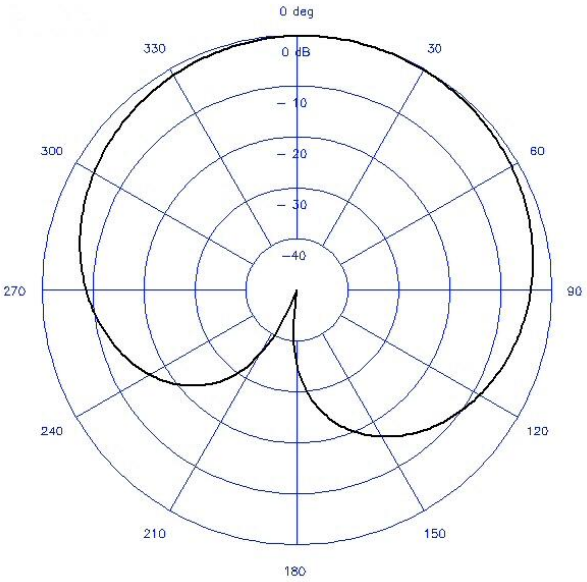

Figure 7. Cardioid pattern obtained with coefficients from Table 1

Azimuth localization can now be carried out in two stages. The first is to calculate and store sets of array weighting coefficients that form cardioid patterns that can be steered through 360° in a predetermines sequence of steps. In the simulations carried out to date, steps of 15° have been found adequate, but this will be re-evaluated using real data following the trials.

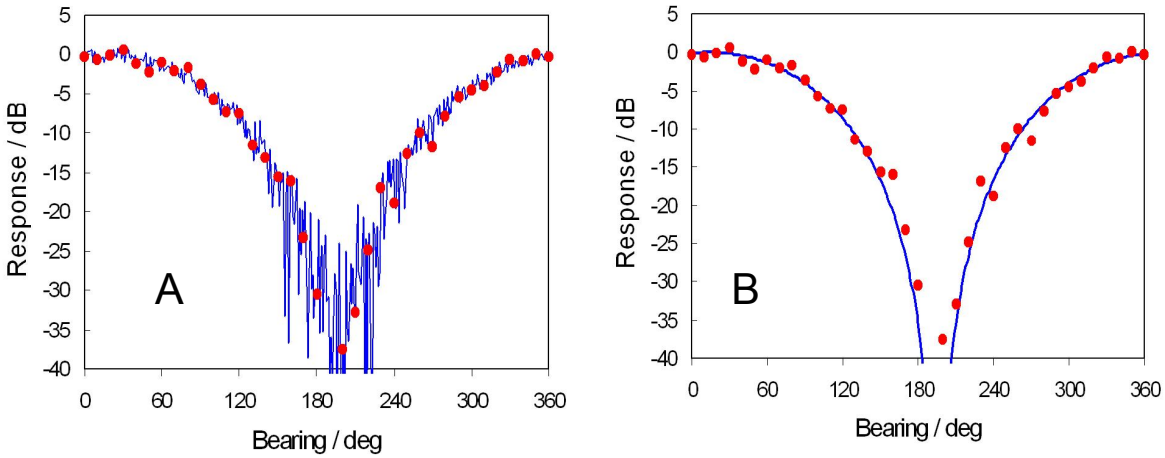

Figure 8. Response of cardioid beamformer to noisy signals (A) and reconstructed cardioid (B) using a least-squares fit to the data points shown as red dots.

The second part of the process is the determination of the direction of arrival of a received signal from the outputs from this rotating sequence of cardioid patterns.

A typical response to simulated noisy signals is shown in Figure 8. The signals are the same as those used to generate Figure 3 with -20dB SNR, and the array output is followed by a matched filter. It is worth noting that the cardioid gives a gain of about 4.5dB which, combined with the gain of the matched filter allows reliable detection at very low SNRs.

In Figure 8A, the beamformer output is plotted against null steer direction as the solid line. It is seen that noise has made it difficult to locate the null precisely. However, the form of the noise-free cardioid response is known and a selection of points from the data (dots) can be used in a least-squares fit to find the parameters needed to reconstruct the cardioid pattern and locate the null direction, as shown in Figure 8B.

The true bearing of the simulated signal was 195° and, in this case, the reconstructed cardioid gives a null steered to 194.6°.

It is noted that this simulation used fixed, frequency independent weighting coefficients, derived for a frequency of 10kHz, approximately the centre frequency of the dolphin whistles. Clearly, this gives a cardioid pattern with a well-defined null over a wide enough band to determine the null direction in the example case. The possibility of using frequency varying coefficients implemented using an FIR filter will be investigated to see if localization accuracy can be maintained with lower SNRs.

Finally, for comparison with Figure 3, the result shown in Figure 8 was repeated 100 times, with a new realisation of the noise background for each repetition, and the histogram of the bearing estimates is plotted in Figure 9. This time the mean bearing estimate is 195.06° with a standard deviation of 0.47° and an overall spread of about 3°.

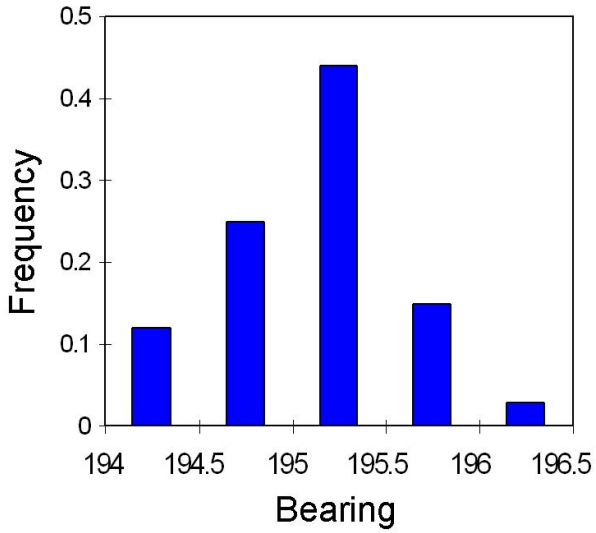

Figure 9. Distribution of bearing estimates obtained with the CBF cardioid with the same signal parameters as Figure 3.

5 CONCLUSIONS

In this paper, simulated results have been used to demonstrate that:

- A rotating cardioid can be used to determine direction of an acoustic source.

- A rotating cardioid can be created using a small three-element array.
- The effects of noise can be overcome by reconstructing the original cardioid using a least-squares fit to the noisy data..
- Azimuth localization of dolphin whistles is feasible with an acoustically small array.

REFERENCES

1. Lepper, P.A., K. Kaschner, P.R. Connelly, and A.D. Goodson, 'Developmentof a simplified ray path model for estimating the range and depth of vocalising marine mammals', *Proc. Inst. Acoust.*, 19(9), 227-234 (1997)
2. Aubauer, R., M.O. Lammers, and W.W.L. Au, 'One-hydrophone method of estimating distance and depth of phonating dolphins in shallow water', *The Journal of the Acoustical Society of America*, 107(5), 2744-2749 (2000)
3. Norris, J., W. Evans, T. Sparks, and R. Benson, 'The use of passive towed arrays for surveying marine mammals', *The Journal of the Acoustical Society of America*, 97(5), 3353 (1995)
4. Thode, A., E.S. Howarth, A. Martinez, and J. Stamates, 'Automated two-dimensional passive tracking of free-ranging dolphins using two towed arrays and frequency-domain beamforming', *The Journal of the Acoustical Society of America*, 112(5), 2399 (2002)
5. Howarth, E.S. and R.H. Defran, 'A sonobouy array for two-dimensional location of dolphin vocalizations', *The Journal of the Acoustical Society of America*, 102(5), 3179-3180 (1997)
6. Tiemann, C.O., M.B. Porter, and L.N. Frazer, 'Automated model-based localization of marine mammals near Hawaii', in *Oceans 2001 MTS/IEEE: An Ocean Odyssey, Vols 1-4, Conference Proceedings.* 2001. p. 1395-1400.
7. White, P.R., D.C. Finfer, T.G. Leighton, C. Powles, and O.N. Baumann, 'Localisation of Whales using Acoustics', *Proc. Inst. Acoust.*, 28(1), 48-59 (2006)
8. Caldwell, M.C. and D.K. Caldwell, 'Individualized Whistle Contours in Bottle-nosed Dolphins (Tursiops truncatus)', *Nature*, 207, 434-435 (1965)
9. Au, W.W.L., *The Sonar of Dolphins*, Springer-Verlag (1993)
10. Oswald, J.N., S. Rankin, and J. Barlow, 'The effect of recording and analysis bandwidth on acoustic identification of delphinid species', *Journal of the Acoustical Society of America*, 116(5), 3178-3185 (2004)
11. Donnelly, M. 'Measuring Seabed Reflection Loss from Ambient Noise: an Experiment in the North-West Approaches to the UK' in *Proc. Seventh European Conference on Underwater Acoustics, ECUA.* 2004. Delft, The Netherlands.
12. Dobbins, P.F., P. Blondel, N.G. Pace, and I. Karasalo. 'SITAR - Localisation and Imaging of Seafloor Targets with Multiple Aspect Scattering' in *Proc. Tenth International Congress on Sound and Vibration ICSV10.* 2003. Stockholm, Sweden.
13. Dobbins, P.F., 'Port/Starboard Discrimination with Towed Arrays', *Proc. Inst. Acoust.*, 18(5), 193-202 (1996)
14. Sayigh, L.S., P.L. Tyack, R.S. Wells, and M.D. Scott, 'Signature Whistles of Free-Ranging Bottlenose-Dolphins Tursiops-Truncatus - Stability and Mother Offspring Comparisons', *Behavioral Ecology and Sociobiology*, 26(4), 247-260 (1990)
15. Sayigh, L.S., P.L. Tyack, R.S. Wells, M.D. Scott, and A.B. Irvine, 'Sex Difference in Signature Whistle Production of Free-Ranging Bottle-Nosed Dolphins, Tursiops-Truncatus', *Behavioral Ecology and Sociobiology*, 36(3), 171-177 (1995)
16. Sayigh, L.S., P.L. Tyack, R.S. Wells, A.R. Solow, M.D. Scott, and A.B. Irvine, 'Individual recognition in wild bottlenose dolphins: a field test using playback experiments', *Animal Behaviour*, 57, 41-50 (1999)
17. Le-Ngoc, S. and T. Le-Ngoc, 'Precision Direction Finding Antennas', *IEEE Trans. Consumer Electronics*, 36(4), 918-921 (1990)
18. Dobbins, P.F. and G.J. Heald. 'General Radiation Pattern Synthesis Technique for Sonar Transducer Arrays'. in *Proc. UDT* 1994 p206-210.